Correlation Effects in Strain-Induced Quantum Dots

R. Rinaldi[1]) (a), M. DeVittorio (a), R. Cingolani (a), U. Hohenester (b),
E. Molinari (b), H. Lipsanen (c), J. Tulkki (c), J. Ahopelto (d), K. Uchida (e),
N. Miura (e), and Y. Arakawa (f)

(a) Istituto Nazionale per la Fisica della Materia (INFM) and Dipartimento di Ingegneria dell'Innovazione, Universiţi Lecce, via Arnesano, I-73100 Lecce, Italy

(b) INFM and Dipartimento di Fisica, Universiţi Modena e Reggio E., via Campi 213/A, I-41100 Modena, Italy

(c) Optoelectronics Laboratory and Laboratory of Computational Engineering, Helsinki University of Technology, Otakaari 7A, P.O. Box 3000, FIN-02015 HUT, Finland

(d) VTT Electronics, Tekniikantie 17, P.O. Box 1101, FIN-02044 VTT, Finland

(e) MegaGauss Laboratory, Institute for Solid State Physics, University of Tokyo, Minato-ku, Japan

(f) Institute of Industrial Science, University of Tokyo, Japan

We report on Coulomb correlation effects in the luminescence of strain-induced quantum dots. In single dots, under low power excitation, we observe the rising of sharp lines associated to the formation of excitonic molecules. In the grand-ensemble, in magnetic fields up to 45 T, we observe Darwin-Fock states of the dots to merge into a unique Landau level, with a considerable reduction in the total diamagnetic shift due to the enhanced electron–hole correlation caused by the increased degeneracy of the state.

1. Introduction The realization of high quality semiconductor quantum dots has recently led to the demonstration of artificial atoms, in which addition energies [1] and Zeeman splitting [2] associated to three-dimensionally confined electron states mimic the characteristics of natural atoms. Similarly, the optical excitation of a single quantum dot (QD) results in optical spectra reminiscent of atomic transitions with sharp and spectrally narrow lines [3–7]. As in the case of atomic and molecular physics the role of Coulomb and exchange interaction is very important for the determination of electronic levels in both multi-electron atoms and molecules and molecular complexes. In this frame, correlation effects can be investigated either in the single dot limit, to explore the formation of multiexciton complexes, or in the grand-ensemble of dots under strong magnetic fields, to clarify the role of wavefunction squeezing and enhancement of the electron–hole correlation due to the high degeneracy.

2. Experimental The investigated samples were strain-induced quantum dots grown by metal-organic vapor phase epitaxy (MOVPE) at atmospheric pressure. The quantum dots (QD) consist of a 8 nm thick $In_{0.2}Ga_{0.8}As$ quantum well (QW) buried by a GaAs barrier of thickness ranging between 5 and 20 nm. Self-organized InP islands (stressors)

---
[1]) Fax:+39-0832-326351; e-mail:ross.rinaldi@unile.it

are grown on the GaAs surface in order to induce a parabolic-like strain potential which laterally confines the carriers in the InGaAs QW underneath the stressor. Details on the samples can be found in Refs. [8, 9]. To isolate a single dot, a square window of 10×10 μm^2 was first opened into a gold mask deposited on the sample surface by UV lithography and lift-off. Then a 200×200 nm^2 mesa, containing a single quantum dot, was defined by AFM lithography and HCl wet chemical etching at the center of the 10×10 μm^2 window. A confocal micro-PL set-up was used to measure each nanomesa. The spectral resolution of the experiments was of the order of 0.7 meV. The magnetoluminescence measurements were performed by inserting the sample in a pulsed-resistive magnet, operating between 0 and 45 T at 4 K. The sample excitation (514.5 nm Ar$^+$ line) and collection were provided by an optical fiber.

3. Results and Discussion

3.1 Effects of correlation on the atomic-like levels of a single parabolic quantum dot
The intensity dependent micro-PL spectra of the single dot isolated in the mesa is shown in Fig. 1, in the energy range of the dot emission. At low photoexcitation power, the full-width at half-maximum of the observed lines is of the order of 0.8 meV. Even though such a linewidth is comparable to the spectral resolution of the experiment and is limited by the sample temperature (about 25 K), we believe that the relatively large linewidth is typical of single QD structures fabricated starting from an InGaAs quantum well, where photoexcited surface charges or near surface impurity states can generate fluctuations of the QD potential in time [10, 11]. In our case, the ground level wavefunction probes small compositional fluctuations in the ternary alloy well underneath the InP dot, where surface charges can eventually accumulate and affect the dots buried under the stressor. (These effects are amplified and can even worsen the PL linewidth when dots are not insulated and neighboring dots can be simultaneously populated due to carrier diffusion [11][2])). In a single-particle picture, we can say that at the lowest density only the ground state 1Σ is populated. This state has twofold degeneracy, and therefore can host up to two electrons and two holes with antiparallel spins. The sharp lines X_0 and B_0, that are split by about 1.5 meV, can then be tentatively associated to the single-exciton and the biexciton level resulting from their interaction. With increasing excitation density the B_0 line becomes dominant, red shifts and broadens, probably overwhelming an additional low energy line (B_1 see below). In any case, with increasing the number of excitons in the dot, its emission intensity raises superlinearly. When the 1Σ-related emission lines saturate, the emission from the first excited state increases. Also in the 1Π emission we note an asymmetry in the low energy tail of the line, due to the contribution of different multi-exciton lines. In this case we cannot resolve the different contributions due to the higher number of interacting particles that populate the first excited state (four electrons and four holes). A similar behavior is observed when the second and third excited states start to be populated with increasing photoexcitation density. Note that the peaks are strongly asymmetric, indicating that they originate from the convolution of several lines[3]), as

---

[2]) μm-PL experiments performed on a single self-assembled QD at 1.2 K showed the same excitation intensity dependence of the emission lines but with narrower linewidth, see e.g. [12].

[3]) At higher photoexcitation intensities a strong broadening is observed. This is probably associated to strong coupling with states in the QW continuum.
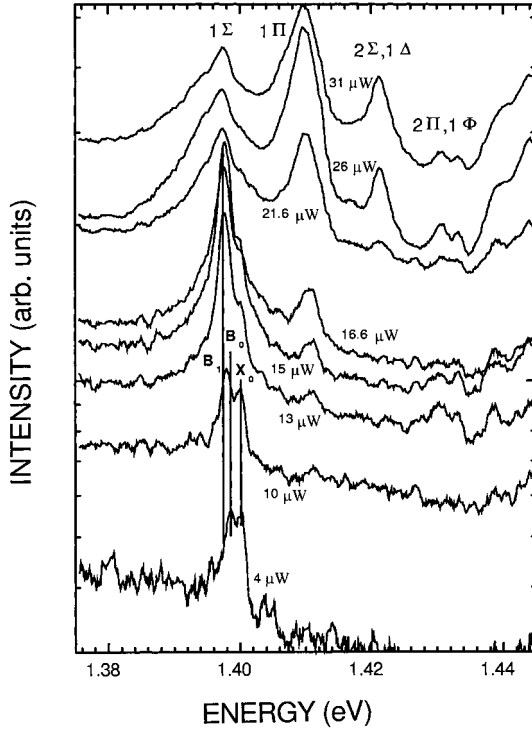
Fig. 1. Microluminescence spectra of the sample with a single quantum dot isolated in a mesa, plotted for different values of photoexcitation power at 20 K

opposed to the perfect Gaussian shape of the peaks in the space-integrated PL [9], associated to inhomogeneous broadening due to the dot size distribution. To understand the origin of the observed lines, we introduce a description of the luminescence process that takes into account the interaction between e–h pairs. The luminescence spectrum $I(\omega)$ can be computed as [13]

$$I(\omega) \propto \sum_{n, n'} f_T(E_n^N) \, |\langle n'; N-1| \, \hat{\pi} \, |n; N\rangle|^2 \times \mathcal{D}_\gamma(\omega - E_n^N + E_{n'}^{N-1}) \,. \tag{1}$$

Here $|n; N\rangle$ is the n-th excited state of the interacting electron–hole system with energy E_n^N (N being the number of e–h pairs), $\mathcal{D}_\gamma(\omega) = 2\gamma/(\omega^2 + \gamma^2)$ with the phenomenological damping constant γ accounting for interactions with the QD environment (e.g., phonons or fluctuations of the electric fields), and $\hat{\pi}$ is the interband polarization operator describing the light–matter coupling within the usual dipole and rotating-wave approximations. In Eq. (1) we have assumed that before photon emission the interacting electron–hole states are occupied thermally according to Boltzmann's distribution at temperature T, $f_T(E)$. Details on calculation are reported in Ref. [14]. Figure 2 shows the luminescence spectra for an increasing number of e–h pairs, N, as computed from Eq. (1). For a single electron–hole pair confined in the QD (Fig. 2a), the luminescence originates from the decay of the groundstate exciton (X_0). For two electron–hole pairs (Fig. 2b) we observe the appearance of the biexcitonic line which is shifted by ~1.5 meV to lower energies (B_0); because of the finite temperature ($T = 25$ K) considered in our calculations, an additional small peak appears at lower photon energy attributed to the decay of a biexcitonic resonance (B_1). For even higher exciton concentrations (Figs. 2c–e) we observe luminescence from both the 1Σ and 1Π shells. In stationary condition experiments, one is averaging over an ensemble of configurations with different numbers of excitons. As a function of increasing photoexcitation density,
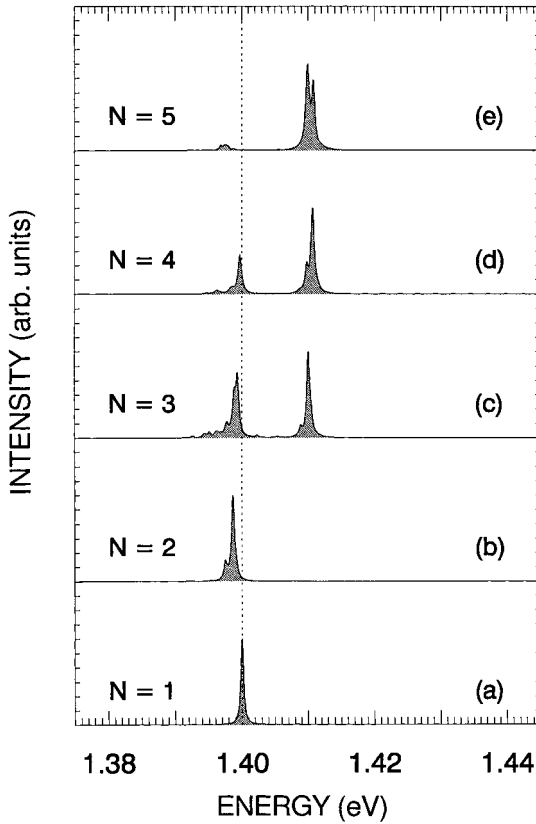
Fig. 2. Luminescence spectra for an increasing number of excitons N as computed from Eq. (1); we use $T = 25$ K and $\gamma = 0.25$ meV. Photon energy zero has been chosen according to the energy of the groundstate exciton. In our calculations we assume, for simplicity, that the interacting electron–hole states consist of optically allowed excitons, X (i.e., excitons where electrons and holes have anti-parallel spin orientations). More specifically, we assume: a) 1X; b) $1X_\uparrow$, $1X_\downarrow$; c) $2X_\uparrow$, $1X_\downarrow$; d) mixture between $2X_\uparrow$, $2X_\downarrow$ and $3X_\uparrow$, $1X_\downarrow$; e) $3X_\uparrow$, $2X_\downarrow$

this ensemble average involves increasing contributions from spectra with higher number of excitons, N. Therefore, the evolution with power in the experimental spectra below 20 μW (Fig. 1) can be interpreted in terms of increasing contributions from the spectra shown in Figs. 2b to e. The good agreement between experiment and theory confirms that confinement induces not only a strong exciton binding, but also a significant coupling between excitons, that is essential to describe the spectral changes as the number of e–h pairs is increased.

3.2 Correlation effects in parabolic quantum dots under high magnetic fields

In Fig. 3 we show the typical evolution of the PL spectra of a QDs ensemble under magnetic field perpendicular to the QW layer with
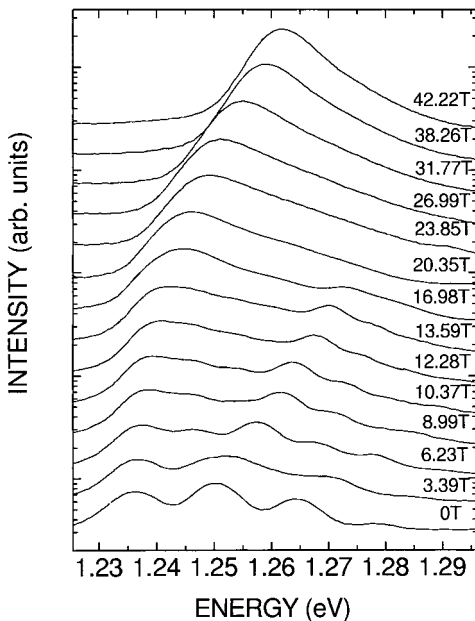

Fig. 3. Magnetoluminescence spectra of the InGaAs strain-induced quantum dot sample, in the energy range of the quantum dot emission
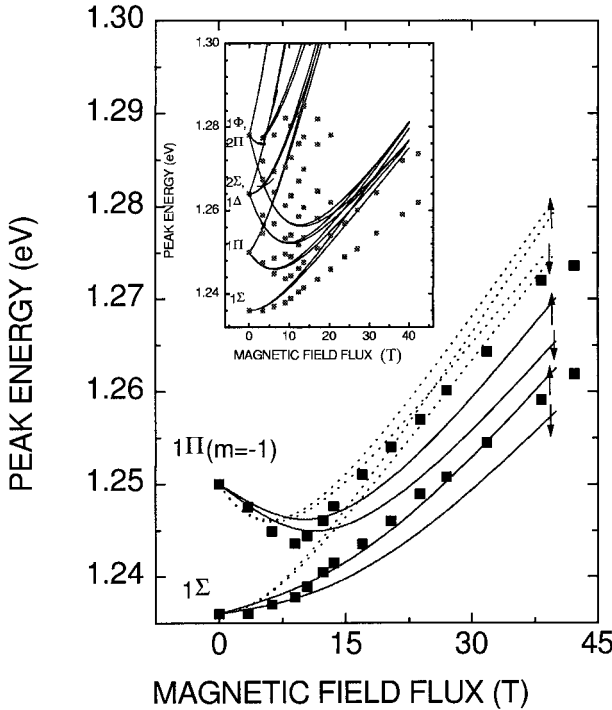
Fig. 4. Comparison between the experimental diamagnetic shift of the ground Landau level (consisting of the 1Σ and $m < 0$ 1Π transitions), and the theoretical shift calculated in the four-band single-particle approximation (dotted curves) or in the full Hartree-Fock model taking into account the electron–hole correlation effects (continuous curves). The symbols $\uparrow$ and $\downarrow$ on the curves indicate the spin orientation. Inset: comparison between the experimental data (symbols) and the calculated (lines) single-particle magnetic field dependence of the ground (1Σ) and excited (1Π, 2Σ, 2Π) quantum dots states

a population of about $N_{e-h} = 6, 8$ per dot. The photoluminescence of the QW between adjacent dots was recorded under the same experimental conditions in the energy range 1.26–1.38 eV. With increasing magnetic field flux the excited QD states broaden and split into two or more lines of different amplitude and width, depending on the value of the angular momentum quantum number. For fields higher than 20 T, all the splitted quantum dot levels merge into two main bands, which narrow and form the quantum dot Landau levels. At higher fields the higher energy Landau level disappears and a strong increase of the QW luminescence intensity is observed, due to carrier spill-over from the higher dot states into the quantum well continuum. In order to obtain the complete fan-plot of all the transitions, shown in the inset of Fig. 4, we have processed each QD and QW magnetoluminescence spectrum by a Gaussian deconvolution [9]. The lifting of degeneracy of the excited states (Zeeman effect) is clearly observable at low fields. At high fields the 1Σ state and the states with $m < 0$ merge into the lowest QD Landau level (1Σ), whereas the higher energy levels ($n\Sigma$, with $n > 1$ or states with $m > 0$) feed the lowest QW Landau level. The Darwin-Fock states in the dots were analyzed by the single-particle Luttinger-Kohn[4]) [9, 15, 16] method as well as by the effective mass many-electron many-hole Hartree-Fock method, whereas the influence of the direct and exchange Coulomb interaction on the magnetic dispersion of

---

[4]) Because of the axial symmetry, the z-component of the total angular momentum $J_{tot} = S_z + L_z$, is a constant of motion for both electrons and holes. Thus, the single particle carrier states can be labeled by $n\Sigma_{\uparrow\downarrow}$, $n\Pi_{\uparrow\downarrow}^{\pm}$, $n\Delta_{\uparrow\downarrow}^{\pm}$, ... where we use $\Sigma, \Pi, \Delta, \Phi, ..$ for quantum number $m = 0, \pm1, \pm2, \pm3, \pm4, ..$, n is the principal quantum number and $\uparrow$ ($\downarrow$) indicates the spin up (down).

luminescence as a function of the number of confined carriers was studied by the Hartree-Fock method [17]. In Ref. [9] we showed that a single-particle four band model describes the diamagnetic shift and the Zeeman splitting of the parabolic quantum dots for magnetic field fluxes up to 10 T. In the present experiment, we find that the single-particle model fails above 10 T, i.e. when the magnetic confinement becomes comparable to the strain-induced potential. Therefore, it is no longer possible to neglect the electron–electron, electron–hole and hole–hole interactions which are enhanced in the squeezed carrier states. This is clearly shown in Fig. 4, where the single-particle diamagnetic shift overestimates the experiment by a steadily increasing amount, for field strengths higher than 20 T. The description of the experimental data improves substantially if we take into account the effects of electron–electron and electron–hole correlation evaluated in the Hartree-Fock approximation [17]. The calculated total diamagnetic shift (continuous lines) reproduces the experimental shift also at very high fields, as opposed to the single particle model (dashed lines). The overall decrease of the electron–hole pair energy due to correlation effects amounts to approximately 20 meV at 40 T, i.e. larger than the interband splitting of the confined states of the dots. The presented Hartree-Fock calculations extend up to $N_{e-h} = 8$. A comparison between calculations including six and eight electron–hole pairs indicates that the combined direct and exchange Coulomb effect saturates with increasing the number of confined carriers.

4. Conclusions   In conclusion, we have investigated the effects of correlation in strain-induced quantum dots. In a single quantum dot the effects of correlation can explain the existence of exciton and biexciton sharp lines in the micro-PL spectra. Under high magnetic fields the single-particle picture fails and the electron–hole correlation must be taken into account in order to reproduce the observed shift.

References

[1] S. Tarucha et al., Phys. Rev. Lett. **77**, 3613 (1996).
    R. C. Ashoori, Nature **379**, 413 (1996).
[2] R. Rinaldi et al., Phys. Rev. Lett. **77**, 342 (1996).
    R. Rinaldi, Int. J. Mod. Phys. B **12**, 471 (1998).
[3] K. Brunner et al., Phys. Rev. Lett. **69**, 3216 (1992).
[4] J.-Y. Marzin et al., Phys. Rev. Lett. **73**, 716 (1994).
[5] A. Kuther et al., Phys. Rev. B **58**, R7508 (1998).
[6] H. Kamada et al., Phys. Rev. B **58**, 16243 (1998).
[7] A. Zrenner et al., Physica B **256–258**, 300 (1998).
[8] H. Lipsanen et al., Phys. Rev. B **51**, 13868 (1995).
[9] R. Rinaldi et al., Phys. Rev. B **57**, 9763 (1998).
[10] M. Bayer et al., Phys. Rev. B **58**, 4740 (1998).
[11] C. Obermüller et al., Appl. Phys. Lett. **74**, 21 (1999).
[12] M. Bayer et al. Nature **405**, 923 (2000).
[13] L. Jacak et al., Quantum Dots, Springer-Verlag, Berlin 1998.
[14] R. Rinaldi et al., Phys. Rev. B **62**, 1592 (2000).
[15] M. Braskén et al., Phys. Rev. B **55**, 9275 (1997).
[16] S. Raymond et al., Solid State Commun. **101**, 883 (1997).
[17] R. Cingolani et al., Phys. Rev. Lett. **83**, 4832 (1999).
[18] J. Motohisa et al., Solid State Electron. **42**, 1335 (1998).
[19] L. Landin et al., Science **280**, 262 (1998).
[20] E. Dekel et al., Phys. Rev. Lett. **80**, 4991 (1998).